Lindahl, U., Backstrom, G., Hook, M., Thunberg, L., Fransson, L., & Linker, A. (1979) *Proc. Natl. Acad. Sci. U.S.A. 76*, 3198–3202.
Lindahl, U., Backstrom, G., Thunberg, L., & Leder, I. G. (1980) *Proc. Natl. Acad. Sci. U.S.A. 77*, 6551–6555.
Lindahl, U., Backstrom, G., & Thunberg, L. (1983) *J. Biol. Chem. 258*, 9826–9830.
Linhardt, R. J., Fitzgerald, G. L., Cooney, C. L., & Langer, R. (1982a) *Biochim. Biophys. Acta 702*, 197–203.
Linhardt, R. J., Grant, A., Cooney, C. L., & Langer, R. (1982b) *J. Biol. Chem. 257*, 7310–7313.
Linhardt, R. J., Cooney, C. L., Larsen, A., Zannetos, C. A., Tapper, D., & Langer, R. (1984) *Appl. Biochem. Biotechnol. 9*, 42–55.
Linker, A., & Hovingh, P. (1972) *Biochemistry 11*, 563–568.
Linker, A., & Hovingh, P. (1979) in *Heparin: Structure, Cellular Functions and Clinical Applications* (McDuffie, N. M., Ed.) pp 3–24, Academic Press, New York.
Linker, A., & Hovingh, P. (1984) *Carbohydr. Res. 127*, 75–94.
Merchant, Z. M., Kim, Y. S., Rice, K. G., & Linhardt, R. J. (1985) *Biochem. J. 229*, 369–377.
Oosta, G. M., Gardner, W. T., Beeler, D. L., & Rosenberg, R. D. (1981) *Proc. Natl. Acad. Sci. U.S.A. 78*, 829–833.
Ototani, N., & Yosizawa, Z. (1979) *Carbohydr. Res. 70*, 295–306.
Ototani, N., Kikuchi, M., & Yosizawa, Z. (1981) *Carbohydr. Res. 88*, 291–303.
Radoff, S., & Danishefsky, I. (1984) *J. Biol. Chem. 259*, 166–172.
Rice, K. G., Kim, Y. S., Grant, A. C., Merchant, Z. M., & Linhardt, R. J. (1985) *Anal. Biochem.* (in press).
Sharath, M., Weiler, J., Merchant, Z. M., Kim, Y. S., Rice, K. G., & Linhardt, R. J. (1985) *Immunopharmacology 9*, 73–80.
Silverberg, I., Havsmark, B., & Fransson, L. A. (1985) *Carbohydr. Res. 137*, 227–238.
Warnick, C. T., & Linker, A. (1972) *Biochemistry 11*, 568–572.
Yang, V. C., Linhardt, R. J., Bernstein, H., Cooney, C. L., & Langer, R. (1985) *J. Biol. Chem. 260*, 1849–1857.

Segmental Flexibility of Receptor-Bound Immunoglobulin E†

James Slattery, David Holowka, and Barbara Baird*
Department of Chemistry, Baker Laboratory, Cornell University, Ithaca, New York 14853
Received April 15, 1985

ABSTRACT: The segmental flexibility of mouse immunoglobulin E (IgE) bound to its high-affinity receptor on membrane vesicles from rat basophilic leukemia cells was compared to that of IgE in solution by measuring the steady-state anisotropy as a function of temperature and viscosity. A monoclonal IgE was used to bind the fluorescent probe *N*-[5-(dimethylamino)naphthalene-1-sulfonyl]-L-lysine (DNS-Lys) rigidly and specifically in the antigen combining site at the tip of the Fab region. The average rotational correlation time, ϕ, of 74–89 ns for the receptor-bound IgE is only slightly longer than that for IgE in solution where ϕ = 54 ns. Another mouse monoclonal IgE was covalently labeled in the Fab region with *N*-(1-pyrenyl)maleimide. Anisotropy measurements with this derivative yielded results that are very similar to those found with anti-DNS IgE and DNS-Lys. These findings are strikingly different from that expected for a rigid IgE bound to its receptor since in this case ϕ is likely to be very much larger. Evidently, the segmental flexibility of IgE is not greatly altered upon binding to its receptor.

Immunoglobulin E (IgE)[1] is a Y-shaped molecule that binds tightly to its receptor on mast cells and basophils and mediates the triggering of cellular degranulation by multivalent antigen. IgE is analogous to other classes of immunoglobulins, being composed of two heavy (ϵ) chains and two light polypeptide chains that are connected by disulfide bonds and noncovalent interactions. The amino acid sequence of human ϵ (Bennich & von Bahr-Lindstrom, 1974) and DNA sequences of the murine ϵ gene (Ishida et al., 1982; Liu et al., 1982) have shown IgE to have a domain structure similar to other immunoglobulins. IgE is like IgM in that these both exhibit an extra domain, $C_\epsilon 2$ or $C_\mu 2$, in the region corresponding to the hinge of IgG (Dorrington & Bennich, 1978).

A controlling factor in initiating the transmembrane signal is the ability of receptor-bound IgE to be cross-linked by multivalent antigen, and this probably depends on several factors including the flexibility of IgE. In similar situations, the relative abilities of IgG subclasses and IgE to bind antigen and fix complement in solution (Oi et al., 1984) and of IgE to precipitate protein covalently conjugated with hapten (Dudich et al., 1978) have been correlated with their segmental flexibility. Previous studies (Nezlin et al., 1973; Cathou, 1978; Oi et al., 1984) have examined the segmental flexibility of IgE in solution by measuring fluorescence anisotropy. These studies have indicated that IgE is probably less flexible than

† This work was supported by Research Grants AI18306 and AI18610 from the National Institutes of Health.

[1] Abbreviations: DNP, 2,4-dinitrophenyl; DNS, 5-(dimethylamino)-naphthalene-1-sulfonyl; DNS-Lys, DNS-L-lysine; DNP-Lys, DNP-L-lysine; EDTA, ethylenediaminetetraacetate; FWHM, full width at half-maximum; HEPES, *N*-(2-hydroxyethyl)piperazine-*N*′-2-ethanesulfonic acid; HBS, HEPES-buffered saline; Ig, immunoglobulin; Na-DodSO$_4$-PAGE, sodium dodecyl sulfate–polyacrylamide gel electrophoresis; PM, *N*-(1-pyrenyl)maleimide; PM–IgE, anti-DNP-IgE covalently modified with PM; RBL, rat basophilic leukemia; TNP-Cap-Tyr, [[(2,4,6-trinitrophenyl)amino]caproyl]-L-tyrosine; Tris, tris(hydroxymethyl)aminomethane.

0006-2960/85/0424-7810$01.50/0

IgG, although the existence of some segmental motion has been suggested (Nezlin et al., 1973; Cathou, 1978). Because the theoretical anisotropy decay is quite complex, consisting of as many as five exponentials for even a simple ellipsoid (Belford et al., 1972), while measurement of time-dependent decay yields only two or three resolvable components, it has not been possible to precisely define the rotational diffusion constants of immunoglobulins experimentally (Oi et al., 1984). For steady-state anisotropy measurements, only a single average correlation time (ϕ) can be determined (Weber, 1952), so interpretation of results using both methods has been based on the comparison of these empirical correlation times (that are some complex averages of the true correlation times) to the correlation time calculated for a sphere of a hydrodynamically equivalent radius or by comparing correlation times found for proteolytic fragments of the immunoglobulins (Yguerabide et al., 1970; Holowka & Cathou, 1976; Reidler et al., 1982). Recently, another useful comparison has been made to evaluate segmental flexibility: the Fc segment of IgG has been "anchored" by binding of anti-Fc antibodies or by association with staphylococcal protein A (Reidler et al., 1982; Hanson et al., 1985).

We have extended this latter approach in a biologically relevant situation by binding IgE to its Fc receptor on plasma membrane vesicles derived from rat basophilic leukemia (RBL) cells (Holowka & Baird, 1983a). We have employed an anti-DNS monoclonal IgE (Oi et al., 1984) with DNS-Lys bound specifically at the antibody combining sites and also another monoclonal IgE selectively conjugated in the Fab regions with *N*-(1-pyrenyl)maleimide to measure average rotational correlation times by steady-state fluorescence polarization analysis (Perrin, 1926). These correlation times for IgE in solution were compared to that expected for an equivalent sphere and to the correlation times found when Fc was anchored by binding IgE to its receptor on the vesicles. The results of these experiments indicate that IgE retains its segmental flexibility upon binding to membrane receptor.

Experimental Procedures

Characterization of Anti-DNS IgE. Purified murine monoclonal anti-DNS IgE (Oi et al., 1984), a gift of Dr. Jeffry Reidler (Stanford University), was subjected to gel filtration chromatography on a 0.95 $cm^2 \times 70$ cm column of Sephacryl S-300 (Pharmacia) in a HEPES-buffered saline solution containing azide (HBS: 135 mM NaCl, 5 mM KCl, 0.01% NaN_3, and 10 mM HEPES, pH 7.4) at a flow rate of 4.8 mL/h, and 1.0-mL fractions were collected. The column was calibrated with molecular weight standards in the range of 1350–670 000 (Bio-Rad Laboratories). On this column, the anti-DNS IgE runs as a symmetrical band with an apparent molecular weight of 231 000, and fractions from the peak were used in all reported experiments. These fractions were further analyzed by sodium dodecyl sulfate–polyacrylamide gel electrophoresis ($NaDodSO_4$–PAGE). On slab gels containing 12.5% (w/v) acrylamide, the IgE runs as a single band in the absence of reducing agents, and in their presence, IgE runs as two bands: heavy chain (ϵ) and light chain (κ) (Oi et al., 1984). Analytical high-performance gel permeation chromatography was carried out for some samples with a 0.75 × 60 cm Bio-Rad TSK 400 column preequilibrated in 0.1 M sodium sulfate, 0.05 M sodium phosphate, pH 6.8, and 1 mM EDTA.

Preparation and Characterization of N-(1-Pyrenyl)maleimide–IgE (PM–IgE). Murine monoclonal anti-2,4-dinitrophenyl-IgE (Liu et al., 1980) was purified by affinity chromatography as described (Holowka & Metzger, 1982). For some preparations, DNP-L-glycine was removed from anti-DNP combining sites by passage over a column of Bio-Rad AG-1x4 equilibrated with borate-buffered saline at 37 °C (Holowka & Metzger, 1982). All IgE preparations were concentrated with a Millipore CX-30 immersible filter unit, followed by filtration chromatography on a 2 $cm^2 \times 100$ cm column of Sephacryl S-300 in HBS. For modification, a 1-mL sample containing 1 mg of IgE was dialyzed against 50 mM sodium phosphate, pH 8.0, 0.1 M NaCl, and 1 mM EDTA, and then 10 mM *N*-(1-pyrenyl)maleimide (PM) in dimethyl sulfoxide was added to a final concentration of 500 μM [final concentration of dimethyl sulfoxide was 5% (v/v)]. The reaction was carried out at ambient temperature for 2 h while the sample was mixed gently with a Labquake rotator (Labindustries) because of the low solubility of PM. At the end of the reaction time, the sample was spun for 1.5 min at 9000*g* in a Beckman Microfuge B to remove most of the insoluble reagent and then filtered through a Millipore GVWP 01300 filter (0.22-μm) pore size), and this filtrate was passed through a 3-mL centrifuge column (Penefsky, 1977) of Sephadex G-50 equilibrated with phosphate-buffered saline and then dialyzed overnight against HBS. The concentration of PM label on IgE was determined from the absorbance at 343 nm, assuming $\epsilon = 3.75 \times 10^4$ M^{-1} cm^{-1} (Holowka & Hammes, 1976). Correction for absorption by residual DNP in the IgE combining sites was made by subtracting the absorbance at 343 nm before labeling from the absorbance at 343 nm after labeling and accounting for the loss of protein by using the absorbance at 280 nm (the contribution of PM at 280 nm introduces an error of less than 5%). The final IgE concentration was determined from the absorbance at 280 nm by assuming $\epsilon = 1.62$ mL mg^{-1} cm^{-1} for IgE (Liu et al., 1980) and $\epsilon = 1.24 \times 10^4$ M^{-1} cm^{-1} for PM (Holowka & Hammes, 1976). The molecular weight of IgE was assumed to be 184 000 (Liu et al., 1980).

Papain digestion of PM–IgE was carried out as previously described (Holowka & Baird, 1983b) with the following changes: the digestion was stopped by the addition of 0.1 M *N*-ethylmaleimide to a final concentration of 4 mM and cooling the sample to 4 °C for 15 min, then an equal volume of 2% $NaDodSO_4$ (w/v), 20% glycerol (v/v), and 80 mM Tris, pH 6.8, was added, and the sample was boiled for 1.5 min. Slab gels prepared by the method of Laemmli (1970) were employed for $NaDodSO_4$–PAGE as previously described (Holowka & Baird, 1984) to analyze PM–IgE before and after enzymatic digestion (each lane contained 85 μg of IgE). Samples analyzed under reducing conditions were mixed with β-mercaptoethanol to 1% (v/v) and boiled for 1 min immediately prior to electrophoresis. The slabs were examined for fluorescent bands immediately after electrophoresis and also after the protein was fixed by overnight treatment with 10% (v/v) acetic acid and 10% isopropyl alcohol. The fluorescence was excited by using a near-ultraviolet light box equipped with a Corning glass plate CS 7-60 filter. After the fluorescence was examined and marked, the slab gel was treated with Coomassie Brilliant Blue to identify the protein bands.

Preparation of Plasma Membrane Vesicles. These were derived from rat basophilic leukemia cells as described (Holowka & Baird, 1983a) with some modifications as follows. Cells were not preincubated with IgE, and vesiculation was induced by either 50 mM formaldehyde and 1 mM dithiothreitol or 25 mM formaldehyde and 2 mM dithiothreitol. The isolated vesicles were dialyzed at 4 °C overnight against 10 mM sodium phosphate, pH 7.4, 0.15 M NaCl, 0.01% NaN_3, and 1 mM phenylmethanesulfonyl fluoride and then against

HBS. Except where noted, IgE was bound to vesicle receptors by incubating the vesicles (40 pmol of receptors/mL) overnight at 4 °C with the appropriate IgE at 3–5-fold molar excess over receptor concentration. For control samples, vesicles were incubated with an equal amount of buffer and irrelevant mouse IgE, or vesicles were preincubated with a large excess of irrelevant IgE, and then the relevant IgE was added. After incubation, the vesicle suspensions were diluted 10-fold with HBS and centrifuged at 25000*g* for 30 min at 4 °C. The pellets were resuspended in HBS to a final concentration of 50 nM receptor-bound IgE.

Steady-State Fluorescence Anisotropy Measurements. These were made with an SLM 8000 fluorescence spectrophotometer equipped with a double monochromator for excitation and a single monochromator for emission. The emission photomultiplier (Hamamatsu R928) was contained within a cooled housing (EMI-Gencom, Plainview, NY). Excitation light was polarized with Polaroid HNP film, and emitted light was analyzed after passing through a Glan-Thompson calcite prism polarizer. With this instrumental setup, the polarization of 5×10^{-6} M fluorescein in 95% glycerol (v/v) and 5×10^{-3} M NaOH was measured at 325-nm excitation 516-nm emission and at 475-nm excitation, 516-nm emission and found to be −0.140 and 0.376, respectively, in agreement with previous results (Chen & Bowman, 1965). IgE samples were placed in 3 × 3 mm or 1 × 1 cm cuvettes and excited at 340 nm (anti-DNS IgE) or 341 nm (PM–IgE) [bandwidth, 2 nm full width at half-maximum (FWHM)]. Perrin plots (see below) of anti-DNS IgE and PM–IgE in solution were obtained by varying the temperature or by addition of glycerol at 20 °C; for measurements with IgE bound to vesicles, the temperature was always varied. In both cases, viscosities under particular conditions were determined from standard tables (Weast, 1979). The temperature was monitored with a thermocouple (Omega 450 AKT) inserted into the sample and removed before fluorescence measurements were taken. Maintenance of integrity of the vesicle samples under conditions of the anisotropy experiment was checked in the following manner. Samples containing 150 μL of vesicles with ^{125}I-IgE bound to receptors were incubated at 4, 25, and 37 °C for 0.5 h. These were immediately layered onto 200 μL of HBS containing 10% glycerol and centrifuged at 4 °C for 10 min in a Beckman airfuge during which intact vesicles are known to sediment while soluble IgE remains in solution. Under these conditions, >90% of the IgE remained bound to the vesicles, and this was the same for samples incubated at all three temperatures.

For anisotropy measurements of DNS-Lys bound to anti-DNS IgE, 0.07 mg/mL anti-DNS IgE in HBS was placed in a cuvette, and the same volume of buffer was placed in an identical cuvette in order to correct for the background signal. Then the nonpolarized fluorescence emission at 510 nm (16-nm FWHM) was monitored as aliquots of DNS-Lys (Sigma Chemical Co.) were added to both cuvettes until the increasing fluorescence of the sample containing anti-DNS IgE began to level off. Extrapolation of the initial linear part of the titration curve to intersect the asymptote to the curve at high DNS-Lys concentrations indicated the stoichiometry at saturation to be ~1.5 DNS-Lys/IgE. The fluorescence emitted from DNS-Lys in the control sample was found to be 4% of the anti-DNS IgE sample, and controls treated in the same manner but containing irrelevant mouse IgE gave the same results.

For anisotropy measurements of DNS-Lys bound to anti-DNS IgE on vesicle receptors, vesicles were saturated with IgE as described above. This sample was spectrally balanced with a control sample of vesicles containing irrelevant mouse IgE by monitoring the signal from scattered light at 360–400 nm and adding buffer as necessary until the signals were the same, then both samples were titrated with DNS-Lys. Typical emission spectra of these samples are shown in Figure 1A. The difference spectrum (--), obtained by subtracting the spectra of vesicles with anti-DNS IgE bound (---) minus control vesicles with the same amount of DNS-Lys (—), shows how well the samples are matched in the light-scattering region of 360–410 nm. The broad peak centered at 510 nm in the difference spectrum is due to the emission of DNS-Lys in the binding sites of anti-DNS IgE, and this signal was monitored throughout all of the anisotropy measurements. Comparison of the control spectrum in Figure 1A (—) with a spectrum obtained from vesicles alone (not shown) indicates that the DNS-Lys has some fluorescence with an emission maximum at 520–530 nm which is blue-shifted from its spectrum in HBS (not shown), suggesting some nonspecific binding to vesicles, but this amounts to <10% of the emission at 510 nm from DNS-Lys bound to anti-DNS IgE on the vesicles.

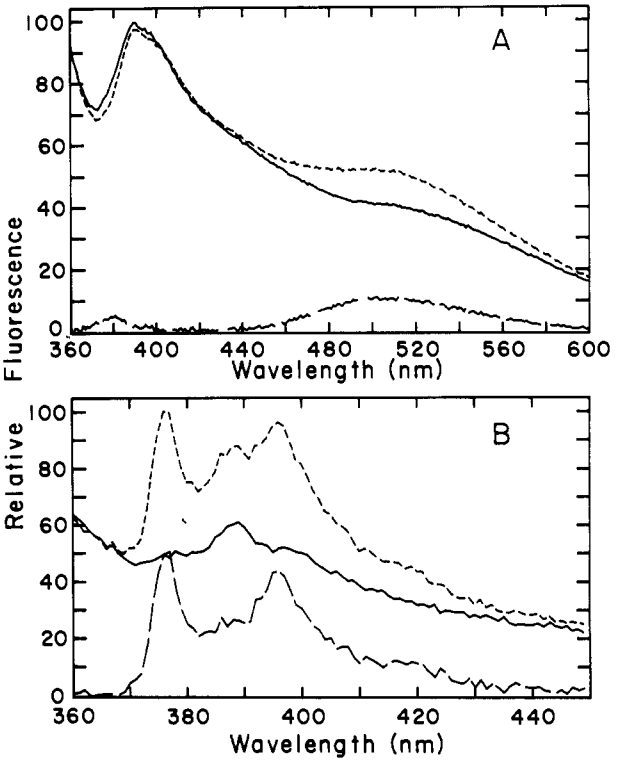

FIGURE 1: Uncorrected fluorescence emission spectra of IgE with fluorescent probes. (A) Excitation at 340 nm: DNS-Lys bound to anti-DNS IgE on vesicles (---); control sample with irrelevant IgE on the vesicles in the presence of the same amount of DNS-Lys (—); difference between the anti-DNS IgE sample and the control (--). (B) Excitation at 341 nm: PM–IgE on vesicles (---); control sample with irrelevant IgE on the vesicles (—); difference between the PM–IgE sample and the control (--). All samples were buffered in HBS.

For anisotropy measurements with PM–IgE, 0.05–0.07 mg/mL was placed in a cuvette, and an equal amount of unlabeled IgE was used for a control. Samples for experiments with IgE bound to receptors on vesicles were prepared as described above; the PM–IgE sample and control vesicle sample were balanced such that the scattered light signal at 350 nm was the same. Typical emission spectra of these vesicles samples are shown in Figure 1B. The spectrum of PM–IgE bound to the vesicles (---) is structured with peaks at 376, 386, and 396 nm and a shoulder at 416 nm, although some detail is lost due to the background signal produced by

the vesicles (—) (the peak at 389 nm in this sample is the Raman peak of water). The peak at 376 nm (4-nm FWHM) was monitored in anisotropy measurements. Proper correction for light scattering is indicated by the very small signal between 360 and 370 nm in the difference spectrum (--) which is what is observed in the spectrum of PM–IgE in solution (not shown).

The steady-state anisotropy, $\bar{A}$, was calculated by using eq 1–4:

$$\bar{A} = \frac{I^{C}_{VV} - GI^{C}_{VH}}{I^{C}_{VV} + 2GI^{C}_{VH}} \quad (1)$$

$$I^{C}_{VV} = I_{VV} - I_{VV}' \quad (2)$$

$$I^{C}_{VH} = I_{VH} - I_{VH}' \quad (3)$$

$$G = I_{HV}/I_{HH} \quad (4)$$

In these equations, I is the emission intensity, and the first and second subscripts refer to the polarization of excitation and emitted light, respectively (vertical and horizontal). I_{VV}' and I_{VH}' are the intensities of the control samples measured at each data point to correct for background fluorescence and light scattering (Shinitzky et al., 1971). In the case of vesicle samples, the light-scattering signal can be significant (Figure 1), and light scattering can also cause depolarization of fluorescence (see Results). The G factor corrects for emission monochromator polarization effects (Chen & Bowman, 1965).

Anisotropy measurements were interpreted by using the Perrin equation (eq 5) (Perrin, 1926) and plotting $\bar{A}^{-1}$ vs. T/η

$$\bar{A}^{-1} = A_0^{-1}(1 + \tau/\phi) = A_0^{-1}(1 + \tau kT/V_n\eta) \quad (5)$$

where T is the temperature in degrees kelvin and η is the viscosity of the solution, A_0 is the limiting anisotropy, τ is the fluorescence lifetime of the probe, k is the Boltzmann constant, and V_h is the hydrated molecular volume. The Perrin equation assumes a spherical molecule holding a rigid fluorophore with a single-exponential lifetime. This formalism was sufficient for interpretation of the anti-DNS IgE data. Since the fluorescence lifetime decay of PM–IgE required a two-exponential fit (see below), the Perrin equation was not applicable and was modified as follows. For a molecule holding m probes with possible different correlation times and for which n possible different fluorescence lifetimes are observed, the relationship between steady-state and time-dependent parameters is given as Brochon et al., 1972; Yguerabide, 1972)

$$\frac{\bar{A}}{A_0} = \frac{\sum_{i=1}^{n}\sum_{j=1}^{m} a_i\tau_i f_j\phi_j/(\phi_j + \tau_i)}{\sum_{i=1}^{n} a_i\tau_i} \quad (6)$$

In this equation, the a_i values are the amplitudes ($\sum a_i = 1$) and the τ_i values are the lifetimes determined when the time decay of fluorescence is expressed as a sum of exponentials. The f_j values are the amplitudes ($\sum f_j = 1$) and the ϕ_j values are the rotational correlation times when the observed anisotropy decay is fit to a sum of exponentials. We approximate PM–IgE to be a rigid probe on a sphere, and we seek a single correlation time (in fact, an average), ϕ, as a function of two fluorescence lifetimes and the steady-state anisotropy parameters $\bar{A}$ and A_0. For this case, eq 6 may be simplified to

$$\frac{\bar{A}}{A_0} = \frac{a_1\tau_1\phi/(\phi + \tau_1) + a_2\tau_2\phi/(\phi + \tau_2)}{a_1\tau_1 + a_2\tau_2} \quad (7)$$

and, solving eq 7 for ϕ:

$$\phi = \left\{\frac{\bar{A}}{A_0}(\tau_1 + \tau_2) - \frac{\tau_1\tau_2}{a_1\tau_1 + a_2\tau_2} \pm \left[\left(\frac{\tau_1\tau_2}{a_1\tau_1 + a_2\tau_2} - \frac{\bar{A}}{A_0}(\tau_1 + \tau_2)\right)^2 + 4\left(1 - \frac{\bar{A}}{A_0}\right)\frac{\bar{A}}{A_0}\tau_1\tau_2\right]^{1/2}\right\} \Big/ [2(1 - \bar{A}/A_0)] \quad (8)$$

Equation 8 was used to calculate an average steady-state correlation time for PM–IgE in solution and bound to vesicles. Only the positive root gives a physically meaningful value.

Steady-State Energy Transfer Measurements. PM–IgE (0.14 μM) in HBS was titrated with 2,4-dinitrophenyl-L-lysine (DNP-Lys), and the decrease in the quantum yield of PM was monitored by the fluorescence at 376 nm after each addition. A similar titration was carried out by using a lower concentration of PM–IgE (0.014 μM) and [[(2,4,6-trinitrophenyl)-amino]caproyl]-L-tyrosine (TNP-Cap-Tyr). Assuming equivalent single donor (PM)-acceptor (DNP or TNP) pairs at saturation, the distance R between the donor and acceptor was calculated according to eq 9 (Förster, 1959):

$$E = 1 - \frac{Q_{DA}}{Q_D} = \frac{(R_0/R)^6}{1 + (R_0/R)^6} \quad (9)$$

For this calculation, Q_{DA}/Q_D was taken as the ratio of the fluorescence of PM–IgE at the end of the titration when all antibody sites were saturated to the fluorescence before any addition of DNP-Lys or TNP-Cap-Tyr. R_0, the critical transfer distance, was calculated as descirbed (Holowka & Baird, 1983a) from independent measurements including the quantum yield of the donor (Q_D) and the donor–acceptor spectral overlap integral (J) and assuming $\kappa^2 = {}^2/_3$. Q_D was determined to be 0.049 with quinine sulfate in 0.1 N H_2SO_4 as a standard. The determination of J used extinction coefficients of DNP-Lys and TNP-Lys bound to IgE which were obtained from appropriate absorption difference spectra.

Measurement of Fluorescence Lifetimes. An Ortec 9200 nanosecond fluorescence spectrophotometer described previously (Matsumoto & Hammes, 1975) was used for these measurements. DNS-Lys bound to anti-DNS IgE was prepared by titration as described above. Samples containing this derivative or the PM–IgE at ambient temperature (23 °C) were excited with light from a spark gap flash lamp that was vertically polarized and passed through a 340-nm Ditric band-pass filter (13.5-nm FWHM). The fluorescence emission was passed through a polarizer either vertically [$V(t)$] of horizontally [$H(t)$] and a 370-nm Ditric band-pass filter (10.8-nm FWHM; Pm–IgE) or a Corning CS-0-51 cutoff filter (50% transmittance at 385 nm; PM–IgE and anti-DNS IgE) before entering the photomultiplier. Collection of $V(t)$ and $H(t)$ was alternated several times throughout the course of the experiment to minimize any instrumental fluctuations; the ratio of $V(t)$ to $H(t)$ determined from total counts during the collection intervals was found not to vary by more than 6%. Scattered light and intrinsic fluorescence produced by unlabeled IgE and nonbound DNS-Lys were corrected by using the controls described above for the steady-state measurements. Decay curves for the controls were recorded separately and subtracted. The lamp pulse, $L(t)$, was recorded from light scattered from a 0.1% Ludox solution after removal of the emission filter. The stability of the lamp was monitored by recording $L(t)$ before, during, and after each IgE sample. The data were analyzed with a PDP 11/24 computer and a nonlinear least-squares fitting procedure (Munro et al., 1979) by convoluting $F(t)$, the time-dependent fluorescence, and $L(t)$

Table I: Steady-State Anisotropy of DNS-Lys Bound to Anti-DNS IgE with Calculated Average Correlation Time (ϕ)

expt	A_0^{-1}	$\bar{A}^{-1}$ [a]	ϕ [b]
Anti-DNS in Solution			
D1	2.54	3.88	54.7
D2	2.53	3.89	53.7
D3[c]	2.51	3.89	52.5
Anti-DNS Bound to Membrane Vesicles			
D4	3.12	4.38	71.5
D5	2.70	3.78	72.1
D6	3.58	4.91	77.6

[a] $T/\eta = 3.35 \times 10^4$ K P^{-1}, $T = 298$ K, and $\eta = 0.008904$ P. [b] Calculated by using eq 5 where $\tau = 28.9$ ns. [c] Isothermal; viscosity altered by addition of glycerol.

to give the experimentally observed decay, $R(t)$, according to eq 10 and 11:

$$R(t) = V(t) + 2H(t) \quad (10)$$

$$F(t) = a_1 e^{-t/\tau_1} + a_2 e^{-t/\tau_2} \qquad a_1 + a_2 = 1 \quad (11)$$

where τ_1 and τ_2 are apparent fluorescence lifetimes. The decay data for DNS-Lys bound to anti-DNS were fit by a single fluorescence lifetime ($a_1 = 1$, $a_2 = 0$ in eq 11). The decay data for PM–IgE required two lifetimes. The normalized root mean squared deviations were less than 0.09 for all fits reported.

Results

Rotational Motion of DNS-Lys Bound to Anti-DNS IgE in Solution and on Vesicles. The steady-state fluorescence anisotropy, A, for DNS-Lys bound to anti-DNS IgE in solution was measured as a function of temperature (T) and viscosity (η) and plotted according to the Perrin equation (eq 5) as shown in Figure 2A. Perrin plots from experiments carried out by varying the temperature (△, ○) or isothermally varying the viscosity by addition of glycerol (■) are collinear, indicating that independent rotation of the probe is not significant (Wahl & Weber, 1967). As listed in Table I, linear least-squares analysis of the individual experiments in Figure 2A provides values for the limiting anisotropy (A_0) and for $\bar{A}$ at 25 °C in buffer contaiing no glycerol ($T/\eta = 3.35 \times 10^4$ K P^{-1}). Extrapolation of the combined data points yields an A_0 of 0.394 which is consistent with a value of 0.384 that was directly measured at the same excitation and emission wavelengths for DNS-Lys bound to anti-DNS IgE in a vitrified solution of 45.7% glycerol (w/w) at 3 °C ($T/\eta = 0.26 \times 10^4$ K P^{-1}). We measured the fluorescence lifetime of DNS-Lys bound to this anti-DNS combining site to be 28.9 ns at 23 °C which is comparable to the value reported previously (25.1 ns at 20 °C; Reidler et al., 1982). By use of this value and the measured values of A_0^{-1} and $\bar{A}^{-1}$ at 25 °C (Table I), eq 5 yields an average rotational correlation time, ϕ, of 54 ± 1 ns, where the error represents the standard deviation of the three experiments listed. It is notable that anisotropy measurements carried out on the anti-DNS preparation prior to gel filtration showed consistently lower values of $\bar{A}$ than those in Figure 2A, and the former measurements yielded significantly higher values of ϕ than those reported in Table I. The explanation for these observations is unclear and in particular does not appear to be due to aggregated IgE, since little, if any, was observed in the Sephacryl S-300 column profile (see Experimental Procedures).

Perrin analyses of three different experiments in which the anti-DNS IgE was bound to high-affinity receptors on membrane vesicles are shown in Figure 2B and Table I. The greater variability in individual data points in these samples compared to the samples with IgE in solution (Figure 2A) can be attributed to poorer statistics caused by a much larger background signal and a smaller DNS signal due to a necessarily lower concentration of bound fluorophore (Figure 1A). Although the points in the individual experiments can be fit with straight lines that are roughly parallel, the values obtained for A_0 are different. This can be explained by Teale's observations (1969) that scattering solutions cause depolarization of fluorescence emission, and, provided the turbidity is temperature independent, the value calculated for the correlation time from linear plots is independent of the effects of light scattering because the emission is depolarized by a constant factor (see below). Table I shows that the data from the three vesicle experiments yield comparable values for ϕ as calculated from eq 5. ϕ averaged over these experiments is 74 ± 3 ns which is only slightly longer than that obtained for DNS-Lys bound to anti-DNS IgE in solution.

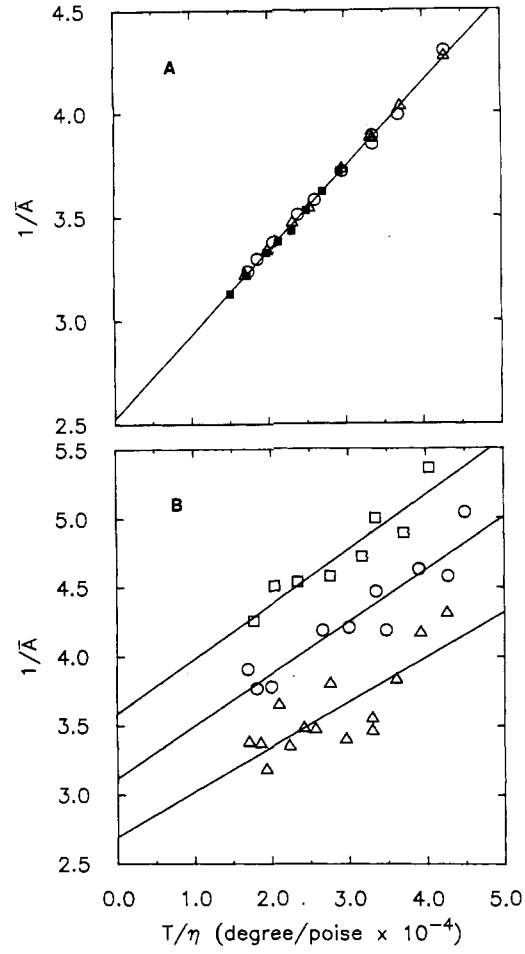

FIGURE 2: Perrin plots of DNS-Lys bound to anti-DNS IgE obtained by varying the temperature except where noted; the experiments are the same as those listed in Table I. (A) Anti-DNS IgE in solution: experiment D1 (○), experiment D2 (△), and experiment D3 (■), carried out isothermally at 20 °C by the addition of glycerol, are fit simultaneously by a single best straight line. (B) Anti-DNS IgE bound to vesicles: experiment D4 (○), experiment D5 (△), and experiment D6 (□) and fit separately with the best straight lines.

Characterization of PM–IgE and Its Rotational Motion in Solution and on Vesicles. Modification of anti-DNP IgE with PM as described under Experimental Procedures resulted in the incorporation of 0.5–1.2 mol of PM/mol of IgE (Table II). Freshly prepared PM–IgE has a fluorescence emission spectrum which resembles that shown in Figure 1B (– –). There is a small but reproducible peak at 386 nm that is consistent with partial intramolecular cross-linking of IgE occurring by aminolysis of the succinimido ring of covalently

Table II: Steady-State Anisotropy and Fluorescence Lifetime Parameters with Calculated Average Correlation Time (ϕ) for Pyrenylmaleimide (PM) Conjugated to Anti-DNP IgE (PM-IgE)[a]

expt	PM/IgE	A_0^{-1}	$\bar{A}^{-1}$[e]	a_1	τ_1 (ns)	a_2	τ_2 (ns)	ϕ (ns)
			PM-IgE in Solution					
P1[c]	0.7[b]	4.00	6.50	0.88	12.7	0.12	89.6	60
P2	0.7[b]	4.03	6.46	0.88	12.7	0.12	89.6	62
P3	0.6[b]	3.88	6.37	0.86	14.0	0.14	89.1	62
P4	0.6[b]	3.99	6.42	0.86	14.0	0.14	89.1	66
P5	0.6[b]	4.06	6.26	0.86	14.0	0.14	89.1	76
			PM-IgE Bound to Membrane Vesicles					
P6	0.5[b]	4.51	8.88	0.84	13.6	0.16	94.2	44
P7	0.8	4.16	6.67	0.84	14.2	0.16	95.4	78
P8	0.8	4.63	6.89	0.84	14.2	0.16	95.4	101
P9	0.8	4.78	7.60	0.84	14.2	0.16	95.4	80
P10[d]	1.2	3.45	5.41	0.83	13.8	0.17	83.7	74

[a] All lifetime data were obtained for PM-IgE in HBS at 23 °C by using the cutoff filter described under Experimental Procedures. Lifetime data were obtained for each PM/IgE stoichiometry and the same data used to calculate ϕ from eq 8 by using data from Perrin plots done on samples of the same age ± 2 days. [b] PM-IgE had residual DNP bound in combining sites (see Experimental Procedures). [c] Isothermal; viscosity altered by addition of glycerol. [d] Control vesicles were preblocked with irrelevant IgE, loaded with PM-IgE, and then spun down as described under Experimental Procedures. [e] $T/\eta = 3.35 \times 10^4$ K P^{-1}, $T = 298$ K, and $\eta = 0.008904$ P.

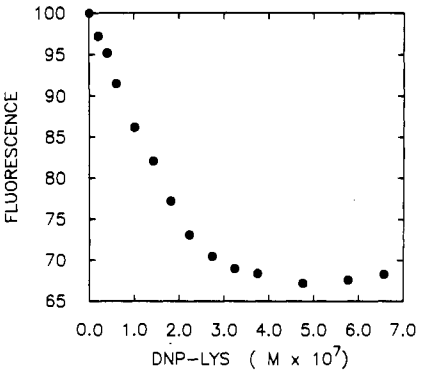

FIGURE 3: Fluorescence quenching data (341-nm excitation, 376-nm emisson) from an experiment measuring energy transfer between PM conjugated to anti-DNP IgE (0.14 μM donor) and DNP-Lys (acceptor) bound to the hapten binding sites as a function of total acceptor concentration.

associated PM (Wu et al., 1976). The relative size of the 386-nm peak gradually increases over several days at pH 8.0 or 7.4 and is apparently not complete after 80 days, suggesting that the participating groups are not oriented for efficient cross-linking. High-performance gel permeation chromatography for an 80-day-old sample showed no dimerization of PM-IgE, ruling out the possibility of intermolecular cross-linking. We also observed a correlation between the increase of the 386-nm peak and a decrease in the fluorescence lifetime (τ) measured for PM-IgE (data not shown). To minimize complications in interpretation of the fluorescence data and calculation of ϕ, PM-IgE samples were used within 2 weeks of their preparation, and anisotropy and lifetime measurements were made within 2 days of each other on any particular sample.

To localize the region on PM-IgE containing the fluorescent label, a preparation lacking DNP-glycine in the antibody combining sites was titrated with specific haptens which act as resonance energy transfer acceptors from donor PM. When DNP-Lys or TNP-Cap-Tyr binds to the anti-DNP combining sites of PM-IgE, there is substantial quenching of PM fluorescence which is maximal at 32% and 20%, respectively. The data for the DNP-Lys titration are shown in Figure 3. The quenching curve is consistent withthe relatively high association constant for DNP-Lys binding to the anti-DNP combining sites of this IgE ($K_a = 2 \times 10^8$ M^{-1}; Liu et al., 1980; J. Erickson, D. Holowka, and B. Baird, unpublished observations). The decrease in the fluorescence lifetime observed when a sample of PM-IgE free of DNP is titrated with DNP-Lys also is consistent with fluorescence energy transfer: the value of $a_1\tau_1 + a_2\tau_2$ was 20% larger for the sample free of DNP-Lys. The R_0 values for energy transfer between PM on IgE and bound DNP-Lys or TNP-Cap-Tyr are calculated to be 24 and 22 Å, respectively, assuming a random orientation of donor and acceptor transition dipoles ($\kappa^2 = {}^2/_3$). By use of the efficiency of energy transfer at saturation (Figure 3) and these values for the R_0's, donor-acceptor distances of 27 Å for DNP-Lys and 28 Å for TNP-Cap-Tyr are calculated from eq 9. Assuming the donor and acceptor transition dipoles are rigidly oriented in parallel ($\kappa^2 = 4$) gives upper limits to the distances as 36 and 38 Å, respectively. Although these calculated values are based on the approximation of a single donor-acceptor pair, which is not necessarily true, they do indicate that a substantial fraction of the PM fluorescence is emitted from probes within the Fab segments, since the antibody combining site is at the tip of this segment that is 80 Å in length (Amzel & Poljak, 1979).

To investigate further the structural location of the PM fluorophores, PM-IgE was digested with papain and analyzed on NaDodSO$_4$-PAGE in the presence of a reducing agent. The pattern of protein bands by Coomassie Brilliant Blue was similar to the papain fragments observed previously for other derivatives of this monoclonal IgE (Holowka & Baird, 1983b) and had major bands at M_r 85K (intact ϵ chain), 76K, 56K, 45K, 36K, 30K (intact κ chain), and 15K. The proteins at M_r 85K, 76K, and 45K showed clearly visible PM fluorescence, while only a trace amount of fluorescence was associated with the 30K and 15K bands and at the dye front. The labeled 45K band probably represents the $V_HC_\epsilon1$ fragment since a similar band is also heavily labeled by fluorescein isothiocyanate and a coumarinylphenylmaleimide under conditions in which these reagents have been shown to preferentially label the Fab region (Holowka & Baird, 1983b; Baird & Holowka, 1985). Notable is the lack of labeling in the M_r 36K band which appears to be $C_\epsilon3C_\epsilon4$ since this fragment is not labeled in the coumarin and fluorescein derivatives of IgE. The lack of detectable fluorescence in the 56K band from PM-IgE is somewhat surprising since it is labeled in the coumarin derivative, but it is consistent with the assignment of this band to be the $C_\epsilon1C_\epsilon2C_\epsilon3$ fragment if most of the PM is localized to the V_H domain (see Discussion). Thus, the papain digestion results support the resonance energy transfer measurements described above and provide further evidence that most of the PM fluorophore is confined to the Fab segments of PM-IgE.

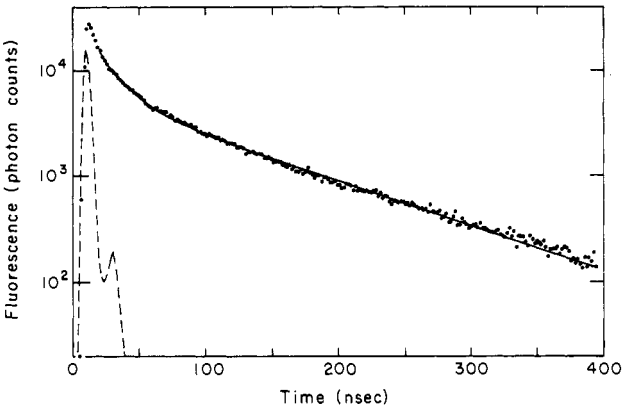

FIGURE 4: Time-dependent fluorescence of PM–IgE at 23 °C in HBS. The experimental data points (●) were fit according to eq 11 (—) by using the best two-exponential decay equation and the lamp pulse profile (---). The fluorescence emission was monitored through a cutoff filter (>385 nm; 50% transmittance at 385 nm).

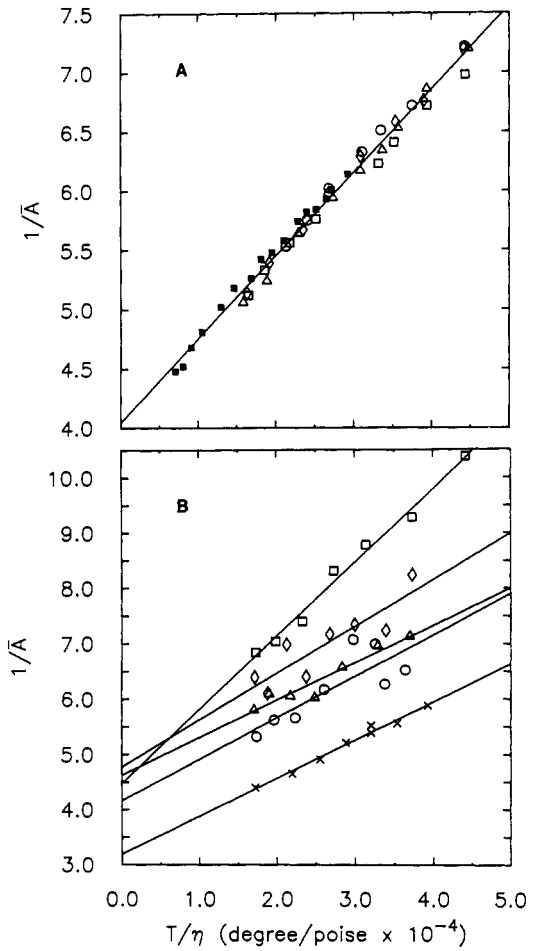

FIGURE 5: Perrin plots of PM–IgE obtained by varying the temperature of samples except where noted; the experiments are the same as those listed in Table II. (A) PM–IgE in solution: experiment P1 (■; carried out isothermally at 20 °C by the addition of glycerol), experiment P2 (○), experiment P3 (△), experiment P4 (◇), and experiment P5 (□) are fit simultaneously with a single best straight line. (B) PM–IgE bound to vesicles: experiments P6 (□), P7 (○), P8 (△), P9 (◇), and P10 (×; control included correction for nonspecifically bound PM–IgE; see text) are fit separately with the best straight lines.

The time-dependent fluorescence of PM–IgE in solution was measured and analyzed in terms of a two-exponential decay as described under Experimental Procedures using eq 10 and 11. Experimental and curve-fitting results from a typical experiment are shown in Figure 4, and the fluorescence lifetimes (τ_1, τ_2) and coefficients (a_1, a_2) are listed for this measurement (P7–P9) and others in Table II.

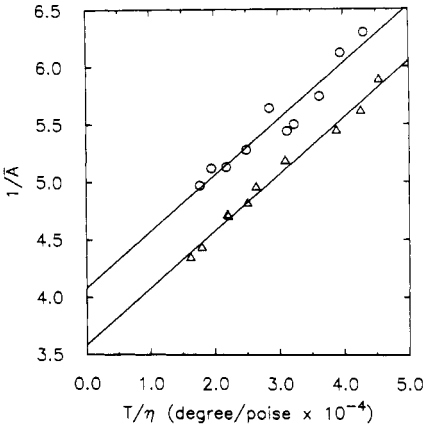

FIGURE 6: Perrin plots of PM–IgE in HBS solution in the absence (△) or presence (○) of vesicles with receptors preblocked by irrelevant IgE. Each set of data points is fit by a best straight line.

Perrin plots of PM–IgE in solution are shown in Figure 5A. T/η was varied by addition of glycerol (■) or by varying T (all other points). There is no apparent discrepancy between the two methods and no curvature of the plots arguing against the possibility of the probe undergoing substantial independent rotation (Wahl & Weber, 1967). Linear least-squares analysis of all the data points gives an A_0 of 0.248. For each experiment, ϕ was calculated by using eq 8 and the corresponding $\bar{A}$, A_0, and fluorescence lifetime data; the results are listed in Table II. These ϕ values range from 60 to 76 ns with an average of 65 ± 5 ns, where the error is the standard deviation of the five experiments.

Perrin analyses of several experiments in which PM–IgE was bound to receptors on the vesicles are shown in Figure 5B and Table II. T/η was varied by adjustment of T in all cases. The control vesicle sample for experiment P10 [(×) in Figure 5B] was pretreated with excess irrelevant IgE and then incubated with PM–IgE and pelleted in order to assess possible nonspecific binding. PM fluorescence in this control was <20% of that for PM–IgE specifically bound to vesicles. As with the anti-DNS IgE bound to vesicles (Figure 2B), there is variability in the extrapolated A_0 among different experiments which is attributed to light scattering as discussed further below. That the lines are less parallel in Figure 5B compared to Figure 2B has possible explanations of heterogeneity in the PM labeling for different PM–IgE preparations or, in the case of P6 [(□) in Figure 5B], complications due to residual DNP in the antibody combining sites (see Discussion). For each experiment, ϕ was calculated by using eq 8 and the corresponding $\bar{A}$, A_0, and lifetime data (Table II). The values for these ϕ range from 45 to 100 ns, a range which includes the values obtained for PM–IgE in solution and DNS-Lys bound to anti-DNS IgE in solution and on vesicles.

Effect of Light Scattering on Fluorescence Depolarization. This effect, described by Teale (1969), was characterized in our system by the following experiment. Two samples of vesicles were incubated overnight with a large excess of irrelevant IgE. Then, without centrifugation, PM–IgE was added to a final concentration of 40 μg/mL to one sample, and an equivalent amount of irrelevant IgE was added to the other which served as the background control. Comparison of these samples showed the scattered light to be about 10% of the signal at the PM–IgE peak (341–nm excitation, 376-nm emission; see Figure 1B). Anisotropy measurements (eq 1–4) made from this set of samples were compared to measurements

made from a second set of samples, one containing 40 μg/mL PM–IgE in solution without any vesicles present with a background control containing 40 μg/mL irrelevant IgE and no vesicles. The temperature was varied to obtain Perrin plots, and they are linear and parallel as shown in Figure 6. These plots yield approximately the same ϕ value (at $T/\eta = 3.35 \times 10^4$ K P^{-1}), since the $\bar{A}/A_0$ ratios are the same within 5% and the fluorescence lifetimes are the same for the two samples (see eq 8). This result indicates that the fluorescence depolarization caused by variable amounts of vesicle-produced light scattering does not significantly affect the measured ϕ in our experiments and additional corrections such as those of Lentz et al. (1979) are unnecessary.

Discussion

The results from this study provide the first experimental evidence that the segmental flexibility exhibited by the Fab arms of IgE in solution is retained at least in part when IgE is bound to its high-affinity receptor. Two separate fluorescent probes were employed on mouse monoclonal IgE in these experiments in order to test for possible artifacts due to low signal to background ratios for the membrane-bound samples or preferential orientation of the transition dipole of the probes. In one case, a monoclonal anti-DNS IgE allowed placement of the probe at the tip of the Fab segments in the antibody combining sites. This is an especially useful location for monitoring the rotation of the Fab region that is tethered to the Fc region at the opposite end of the Fab, ≥80 Å away from the combining site (Dorrington & Bennich, 1978; Amzel & Poljak, 1979). Even though DNS-Lys has a relatively high quantum yield when bound rigidly to the anti-DNS combining site (0.6; Reidler et al., 1982), its low molar extinction coefficient at the long-wavelength absorption band ($\epsilon_{340nm} = 3400$ M^{-1} cm^{-1}; Parker et al., 1967) results in a very weak fluorescence signal for the 10–50 nM concentration range that had to be employed for the vesicle-bound IgE derivatives in these experiments. Steady-state anisotropy measurements were made in the present studies because the signal to background ratio was too low for meaningful nanosecond anisotropy decay measurements using a conventional spark gap lamp.

Segmental Flexibility in Solution. In order to assess segmental flexibility of anti-DNS IgE in the conventional manner, we calculated the correlation time of a rigid spherical particle with hydrodynamic properties similar to those of mouse IgE using two different methods to calculate the equivalent hydrated volume (V_h). The first method uses M_r 184 000 and the partial specific volume ($\bar{v} = 0.715$ cm^{3}g^{-1}) for mouse IgE (Liu et al., 1980) and assumes a minimal value for the hydration of the protein ($h = 0.3$ g of H_2O/g of protein; Cantor & Schimmel, 1980) for substitution into the equation:

$$V_h = (M_r/N_0)(\bar{v} + h\rho) = 4\pi r_e^3/3 \qquad (12)$$

where N_0 is Avogadro's number, ρ is the density of the HBS at 25 °C, and r_e is a hydrodynamically equivalent radius. Using this value for V_h and solving for ϕ in eq 5 yield a minimal rotational correlation time of 78 ns. Equation 13

$$r_e = \frac{M_r(1 - \bar{v}\rho)}{N_0 6\pi\eta s} \qquad (13)$$

provides another way to calculate r_e that does not rely on an estimated h but uses the measured sedimentation coefficient, s (Hanson et al., 1981), which for IgE is 8.2 S (Liu et al., 1980). η is the viscosity of the solution at 25 °C (Table I). The correlation time calculated from this r_e according to eq 12 and 5 is 155 ns. This range of calculated values for the global tumbling of IgE using a spherical approximation is significantly greater than the measured value of 54 ns (Table III), indicating that some internal nodes of motion other than free probe rotation must be contributing to the observed fluorescence depolarization (Yguerabide et al., 1970; Hanson et al., 1981). Since there is no apparent rotation of the probe in the combining site (as indicated by the collinearity of the isothermal and variable-temperature Perrin plots), the possibility of segmental motion within IgE is very likely. By analogy with more detailed analyses carried out on other immunoglobulin classes using antibody fragments (Yguerabide et al., 1970; Holowka & Cathou, 1976), segmental flexibility of the Fab regions of IgE is probably the major contributor to this internal motion.

Table III: Summary of Rotational Correlation Times

sample	average ϕ (ns)[a] in solution	on membranes
DNS-Lys–anti-DNS IgE	54 ± 1 (3)[b]	74 ± 3 (3) to 89[e]
PM–IgE	65 ± 6 (5) to 75[c]	75 ± 20 (5) to 86[c]
IgE, equivalent sphere	78–155[d]	>1000[f]

[a] At 25 °C in HBS. [b] Error represents the standard deviation of the experiments listed in Tables I and II, and the number of experiments is indicated in parentheses. [c] Upper limit of range includes possible error in lifetime determinations (see Discussion). [d] Range of values calculated according to eq 12 and 13 as described under Discussion. [e] Upper limit of range includes possible error due to improper background correction (see Discussion). [f] Assumes rotational motion limited to in-plane rotation of the membrane-bound IgE–receptor complex (see Discussion).

Previous studies on human IgE myeloma proteins using covalently conjugated DNS and either steady-state polarization (Nezlin et al., 1973) or time-resolved fluorescence depolarization methods (Cathou, 1978) suggested that the extent of segmental flexibility in this class of immunoglobulins may be less than that observed of IgG. Similar conclusions were reached by Oi et al. (1984), who compared the nanosecond anisotropy decay of the mouse monoclonal anti-DNS IgE used in the present study to several IgG isotypes with the same combining sites. These authors chose to calculate a weighted average of the two measurable correlation times, which for IgE was 124 ns, and this is within the range of values expected for an equivalent rigid sphere according to eq 12 and 13 (Table III). The average value of ϕ for anti-DNS IgE from the present steady-state polarization measurements (54 ns) is not directly comparable to the average ϕ calculated from the decay data of Oi et al. (1984) [see Hanson et al. (1981)]. Our value may be compared to $\phi = 55$ ns for myeloma IgE and $\phi = 21$–30 ns for IgG obtained with steady-state measurements by Nezlin et al. (1973), although their use of DNS that was covalently conjugated leaves open the possibility of independent rotation of the fluorescent probes which might cause lower apparent values for ϕ. Our value can also be compared with that for a polyclonal anti-DNS IgG from rat, in which the average ϕ from a Perrin analysis of steady-state polarization measurements was found to be 37 ns (Tumerman et al., 1972). Since the calculated correlation time for an equivalent sphere of IgG is about the same as that for IgE (Cathou, 1978; Hanson et al., 1981), the 1.5-fold larger ϕ obtained with anti-DNS IgE in the present study may well reflect some restriction of segmental flexibility relative to that of IgG.

We obtained similar results with PM–IgE in solution. The average rotational correlation time in solution for this derivative is 65 ± 6 ns, which is slightly longer than that obtained with DNS-Lys in the anti-DNS combining sites (Table III). Some part of this discrepancy may be due to differences in the orientation of the transition dipoles of these two probes with respect to the axes of rotational motion. It is noteworthy

that the multiexponential nature of the PM–IgE fluorescence decay required the use of a more complex form of the Perrin equation (eq 8) which was derived to eliminate the use of weighted averages of the fluorescence lifetimes that are generally inadequate for this purpose (Hanson et al., 1981). The fluorescence lifetimes used and listed in Table II were measured by employing a cutoff filter on the emission side, allowing long-wavelength light to pass with a 50% transmittance at 385 nm. Use of this filter may have underestimated the lifetimes of the fluorescence emission at 376 nm, where the steady-state anisotropy measurements were made, since fluorescence decays observed with a band-pass filter at 370 nm resulted in values for a_2 that were 1.0–1.5 times larger and for τ_2 that were 1.1 times longer with no significant change in τ_1. In this case, the values of ϕ listed in Table II may underestimate the actual values, but we conservatively estimate this error to be less than 15%. It is notable that the values of ϕ obtained for PM–IgE in solution with several different preparations listed in Table II, experiments P1–P5, are generally in good agreement, indicating that the calculated ϕ values were not extremely sensitive to small variations in age, labeling stoichiometry, or the presence of intramolecular cross-linking.

The location of the fluorescent probe in PM–IgE is less certain than for DNS-Lys bound to anti-DNS IgE, but both energy transfer measurements to the anti-DNP combining sites and enzymatic cleavage studies indicate that most if not all of the pyrene is confined to the Fab fragment. This is consistent with previous studies using this IgE and other fluorescent alkylating reagents which have shown that there are no free sulfhydryls, yet several of these reagents react selectively with a limited number of residues in the $V_HC_\epsilon1C_\epsilon2$ domains under nonreducing conditions (Baird & Holowka, 1985). Energy transfer from PM to either DNP-Lys or TNP-Cap-Tyr bound in the anti-DNP combining sites indicates that a large fraction of the PM must be within 40 Å of the combining sites. This result is somewhat different than that for the coumarinylphenylmaleimide derivative of anti-DNP IgE in which the fluorescent label appears to be greater than 50 Å from the antibody combining sites and is probably located in the $C_\epsilon1$ domain (Baird & Holowka, 1985). Fluorescent labeling of papain cleavage products is also different for the PM and coumarinylphenylmaleimide derivatives of IgE as analyzed by NaDodSO$_4$–PAGE: in the latter case, the 50–56K band is strongly fluorescent, but with the PM derivative, it is not. In both cases, the 40–45K band that probably represents $V_HC_\epsilon1$ is labeled while the 34–36K band that may be $C_\epsilon3C_\epsilon4$ is not labeled. The labeling patterns and energy transfer data suggest that most of the PM label is in the V_H domain, although some PM labeling of other domains cannot be ruled out. The measured correlation time of 65–75 ns (Table III) for PM–IgE in solution is less than that expected for the global rotation of IgE using a spherical approximation (see above) and is consistent with the presence of segmental flexibility indicated by the experiments with anti-DNS and DNS-Lys.

Segmental Flexibility of Receptor-Bound IgE. Fluorescence anisotropy measurements of DNS-Lys–anti-DNS IgE complexes bound to receptors on membrane vesicles result in values of ϕ about 1.4-fold larger than those obtained for anti-DNS in solution. In three separate experiments, $\phi = 64 \pm 3$ ns was reproducibly determined despite the large amount of scatter in the individual data sets. Systematic errors in this value are most likely to arise from incorrect use of fluorescence lifetimes determined for the IgE in solution or from an improper subtraction of background signal produced by the vesicles. The fluorescence lifetime of a probe could be affected by the conformation of the macromolecule to which is is attached, and there is recent evidence that the conformation of receptor-bound IgE is different than that in solution (Holowka et al., 1985). However, this change is probably localized to the region of the Fc interacting with the receptor, and it is unlikely that the change extends to the combining sites since the affinity of anti-DNP IgE to several haptens is not altered upon IgE binding to its receptor on the cell surface (J. Erickson, D. Holowka, and B. Baird, unpublished results). Furthermore, the quantum yield of PM does not change significantly when PM–IgE binds to receptor (unpublished observations), suggesting there is no significant change in the PM fluorescence lifetime when this derivative binds.

Potential errors in the background correction of the anisotropy measurements are most serious for the anti-DNS experiments since the signal to background ratio is low (see Figure 1A). Light scattering due to the vesicles was matched, but the fluorescence contribution at 510 nm due to nonbound DNS-Lys could have been overcorrected by as much as 10%, since both samples, with and without anti-DNS, contained the same amount of DNS-Lys. This error would result in underestimating ϕ by no more than 20% (Table III). The small error introduced by IgE that is not specifically bound to vesicle receptors (<10%; Holowka & Baird, 1983a) would have no significant effect on the measured correlation time for the receptor-bound IgE, since the value of ϕ for IgE in solution is not very different. The variable shifts in the Perrin plots seen in Figures 2B and 5B for different experiments with membrane-bound IgE do not alter the values obtained for ϕ (Tables I and II). These observations are consistent with the predictions of Teale (1969) for the constant effects of light scattering with respect to temperature on fluorescence depolarization, and the experiment shown in Figure 6 provides direct evidence to support this explanation.

The average rotational correlation time for PM–IgE bound to membrane vesicles is 75 ± 20 ns as shown by the data in Table II. This may underestimate the true value by as much as 15% due to uncertainty in the fluorescence lifetime measurements as described above for PM–IgE in solution. Correction for nonspecifically bound PM–IgE that amounts of <20% of the total fluorescence does not significantly alter the value of ϕ obtained [experiment P10, Figure 5B (×) and Table II]. The reason for greater variability observed among different experiments with PM–IgE on the vesicles than for anti-DNS IgE is unclear, but it may be due to variability among the different preparations of PM–IgE. In the case of experiment P6 [Figure 5B (□) and Table II], some residual DNP was present in the combining sites of the preparation of PM–IgE after purification, and the lifetime measurements were made on this sample in solution. However, when this PM–IgE was bound to the vesicles, washed, and diluted for anisotropy measurements, some DNP probably dissociated, resulting in slightly longer lifetimes than those measured, and therefore, an incorrectly low ϕ would have been calculated by using eq 8. Even accounting for all of these sources of error (uncertainties in lifetimes and background corrections), it is clear that the average rotational correlation time of PM–IgE bound to its receptor is only slightly greater than that determined for this derivative in solution (Table II). Thus, only small increases in the rotational correlation times for both anti-DNS IgE and PM–IgE are observed to result from their binding to high-affinity receptors on plasma membrane vesicles (Table III).

In considering the results of this study, it is useful to cal-

culate roughly the change in ϕ expected for IgE that has no segmental flexibility or loses it upon on binding to receptors on the vesicles. If a rigid IgE is tethered by its C-terminal end but still able to rotate as a whole molecule, then the theory of Wegener et al. (1980) would predict an end over end rotational correlation time for the bound IgE to be 2–3 times greater than that for the free IgE [assuming an axial ratio of 1–5; see D_{free}/D_{fixed} in Figure 2 of Wegener et al. (1980)]. This would represent a lower limit to the expected ϕ since the tight binding of IgE to receptor indicates multipoint attachment such that it is unlikely that unrestricted rotation could occur. It is also unlikely that the membrane-bound receptor itself exhibits any substantial amount of segmental flexibility on the extracellular (IgE binding) side of the membrane, since it is relatively resistant to proteolytic digestion (Metzger et al., 1976). The best comparison may be with the correlation time for the rotation of membrane proteins in the plane of the bilayer which is typically $>10^3$ ns (Austin et al., 1979; Zidovetzki et al., 1981; Cherry, 1979). The global tumbling of an entire membrane vesicle that is ≥ 0.1 μm in diameter should be $>10^5$ ns on the basis of eq 5 and 12. Since we measured ϕ for receptor-bound IgE to be 70–90 ns, this provides strong evidence that receptor-bound IgE exhibits a significant amount of segmental flexibility. Our resonance energy transfer studies on receptor-bound IgE are consistent with the Fc portion bound rigidly to receptor while the Fab arms have some rotational motion (Holowka et al., 1985). In this case, the Fab of receptor-bound IgE may be modeled as an ellipsoid flexibly attached to a fixed point (at the interface with the Fc segment) while the Fab of soluble IgE can be considered as flexibly attached by its C-terminal end to an indentical segment (Fc). It is interesting to note that the predicted increase in the rotational correlation time when IgE binds to receptor in this case is 1.5-fold [assuming an axial ratio of 2 for the Fab; see $D_{\perp}/D_{fixed}$ in Figure 2 of Wegener et al. (1980)] which is within the range of 1.1–1.7-fold that we measure (Table III).

What remains to be determined experimentally is whether the extent of flexibility and the sites of rotational bending and/or twisting are altered due to the interaction of IgE with its receptor. One possible site for this alteration is the junction between the $C_\epsilon 2$ and $C_\epsilon 3$ domains which has been shown to have a decreased susceptibility to trypsin digestion for rat IgE bound to the α subunit of the receptor (Perez-Montfort & Metzger, 1982). The analogous interdomain region in IgM has been inferred to be a site of segmental flexibility in that immunoglobulin (Holowka & Cathou, 1976), and it is proposed that this may be the site of a conformational change that accompanies binding of IgE to its receptor (Holowka et al., 1985). Abolition of segmental flexibility at that site would still leave the junction between $C_\epsilon 1$ and $C_\epsilon 2$ as well as the switch between V_H and $C_\epsilon 1$ (Wrigley et al., 1983) as possible candidates for segmental motion. The increase in ϕ for anti-DNS bound to its receptor compared to anti-DNS in solution might reflect some loss in the possible degrees of freedom of the Fab segments, or it may simply reflect the change in the component of ϕ due to global tumbling of IgE which increases when its Fc segment is tied down to the vehicle (Wegener et al., 1980; Hanson, 1985). Answers to these more detailed questions await measurements of greater sensitivity and time resolution, possibly through the use of a pulsed laser source to observe time-dependent anisotropy decay of the fluorophores attached to IgE.

ACKNOWLEDGMENTS

We are grateful to Dr. Jeffry Reidler for providing us with the purified monoclonal anti-DNS IgE and for advice regarding its use and to Professor Gordon G. Hammes for use of the Ortec nanosecond fluorescence spectrophotometer.

REFERENCES

Amzel, L. M., & Poljak, R. J. (1979) *Annu. Rev. Biochem. 48*, 961–997.

Austin, R. H., Chan, S. S. & Jovin, T. M. (1979) *Proc. Natl. Acad. Sci. U.S.A. 76*, 5650–5654.

Baird, B., & Holowka, D. (1985) *Biochemistry 24*, 6252–6259.

Belford, G. G., Belford, R. L., & Weber, G. (1972) *Proc. Natl. Acad. Sci. U.S.A. 69*, 1392–1393.

Bennich, H., & von Bahr-Lindstrom, H. (1974) in *Progress in Immunology II* (Brent, L., & Hoborrow, J., Eds.) Vol. 1, pp 49–58, North-Holland, Amsterdam.

Brochon, J.-C., Wahl, P., & Auchet, J. C. (1972) *Eur. J. Biochem. 25*, 20–32.

Cantor, C. R., & Schimmel, P. R. (1980) in *Biophysical Chemistry*, p 552, W. H. Freeman, San Francisco, CA.

Cathou, R. E. (1978) *Compr. Immunol. 5*, 37–83.

Chen, R. F., & Bowman, R. L. (1965) *Science (Washington, D.C.) 147*, 729–732.

Cherry, R. J. (1979) *Biochim. Biophys. Acta 559*, 289–327.

Dorrington, K. J., & Bennich, H. (1978) *Immunol. Rev. 41*, 3–25.

Dudich, E. I., Nezlin, R. S., & Franek, F. (1978) *FEBS Lett. 89*, 89–92.

Förster, T. (1959) *Discuss. Faraday Soc. 27*, 7–17.

Hanson, D. C. (1985) *Mol. Immunol. 22*, 245–250.

Hanson, D. C., Yguerabide, J., & Schumaker, V. N. (1981) *Biochemistry 20*, 6842–6852.

Hanson, D. C., & Yguerabide, J., & Schumaker, V. N. (1985) *Mol. Immunol. 22*, 237–244.

Holowka, D., & Cathou, R. E. (1976) *Biochemistry 15*, 3379–3390.

Holowka, D., & Hammes, G. G. (1977) *Biochemistry 16*, 5528–5545.

Holowka, D., & Metzger, H. (1982) *Mol. Immunol. 19*, 219–227.

Holowka, D., & Baird, B. (1983a) *Biochemistry 22*, 3466–3474.

Holowka, D., & Baird, B. (1983b) *Biochemistry 22*, 3475–3484.

Holowka, D., & Baird, B. (1984) *J. Biol. Chem. 259*, 3720–3728.

Holowka, D., Conrad, D. H., & Baird, B. (1985) *Biochemistry 24*, 6260–6267.

Ishida, N., Ueda, S., Hayashida, H., Miyaka, T., & Honjo, T. (1982) *EMBO J. 1*, 1117–1123.

Lentz, B. R., Moore, B. M., & Barrow, D. A. (1979) *Biophys. J. 25*, 489–494.

Liu, F. T., Bohn, J. W., Ferry, E. L., Yamamoto, H., Molinaro, C. A., Sherman, L. A., Klinman, N. R., & Katz, D. H. (1980) *J. Immunol. 124*, 2728–2736.

Matsumoto, S., & Hammes, G. G. (1975) *Biochemistry 14*, 214–224.

Metzger, H., Budman, D., & Lucky, P. (1976) *Immunochemistry 13*, 417–423.

Munro, I., Pecht, I., & Stryer, L. (1979) *Proc. Natl. Acad. Sci. U.S.A. 76*, 56–60.

Nezlin, R. S., Zagyansky, Y. A., Käiväräinen, A. I., & Stefani, D. V. (1973) *Immunochemistry 10*, 681–688.

Oi, V. T., Voung, T. M., Hardy, R. Reidler, J., Dangl, J., Herzenberg, L. A., & Stryer, L. (1984) *Nature (London) 307*, 136–140.

Parker, C. W., Yoo, T. J., Johnson, M. C., & Godt, S. M. (1967) *Biochemistry 6*, 3408–3416.

Penefsky, H. S. (1977) *J. Biol. Chem. 252*, 2891–2899.
Perez-Montfort, R., & Metzger, H. (1982) *Mol. Immunol. 19*, 1113–1125.
Perrin, M. F. (1926) *J. Phys. (Les Ulis, Fr.) 7*, 390–401.
Reidler, J., Oi, V. T., Carlsen, W. Vuong, T. M., Pecht, I., Herzenberg, L. A., & Stryer, L. (1982) *J. Mol. Biol. 158*, 739–746.
Shinitzky, M., Dianoux, A.-C., Gitler, C., & Weber, G. (1971) *Biochemistry 10*, 2106–2113.
Teale, F. W. J. (1969) *Photochem. Photobiol. 10*, 363–374.
Tumerman, L. A., Nezlin, R. S., & Zagyansky, Y. A. (1972) *FEBS Lett. 19*, 290–292.
Wahl, P., & Weber, G. (1967) *J. Mol. Biol. 30*, 371–382.
Weast, R. C., Ed. (1979) *Handbook of Chemistry and Physics*, 60th ed., pp D239 and F51, CRC Press, Boca Raton, FL.
Weber, G. (1952) *Biochem. J. 51*, 155–167.
Wegener, W. A., Dowben, R. M., & Koester, V. J. (1980) *J. Chem. Phys. 73*, 4086–4097.
Wrigley, N. G., Brown, E. B., & Skehel, J. J. (1983) *J. Mol. Biol. 169*, 771–774.
Wu, C.-W., Yarbrough, L. R., & Wu, Y.-H. (1976) *Biochemistry 15*, 2863–2868.
Yguerabide, J. (1972) *Methods Enzymol. 26*, 498–578.
Yguerabide, J., Epstein, H. F., & Stryer, L. (1970) *J. Mol. Biol. 51*, 573–590.
Zidovetzki, R., Yarden, Y., Schlessinger, J., & Jovin, T. M. (1981) *Proc. Natl. Acad. Sci. U.S.A. 78*, 6981–6985.

Analysis of the Specificity of Five Murine Anti-Blood Group A Monoclonal Antibodies, Including One That Identifies Type 3 and Type 4 A Determinants†

Koichi Furukawa,‡ Henrik Clausen,§ Sen-itiroh Hakomori,§ Junichi Sakamoto,‡ Katherine Look,‡ Arne Lundblad,‖ M. Jules Mattes,‡ and Kenneth O. Lloyd*,‡

Memorial Sloan-Kettering Cancer Center, New York, New York 10021, Fred Hutchinson Cancer Center, Seattle, Washington 98104, and University of Lund, S-22185 Lund, Sweden

Received May 29, 1985

ABSTRACT: The specificity of five mouse monoclonal anti-A blood group antibodies (Ab), four of which were produced by immunization with cultured human cancer cells and one with a synthetic antigen, has been determined by examining their reactivity with purified A glycolipids, erythrocyte glycolipids, oligosaccharides, ovarian cyst glycoproteins, and salivary glycoproteins. Two of the antibodies (HT29-36 and CB) reacted with all A variant structures tested and have a broad anti-A reactivity. Ab CLH6 did not agglutinate A erythrocytes and reacted preferentially with the type 1A structure. Ab S12 agglutinated all A_1 erythrocytes and reacted best with simple, monofucosyl type 2 A structures, such as A^a-2, A^b-2, and A tetrasaccharide. Ab M2 has a novel, but complex, spectrum of reactivity. It reacts with type 3 and type 4 A chains and not with type 1 and type 2 A chains. It appears to recognize both an external A structure

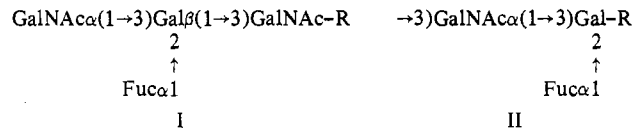

(I) (found) in type 3 and type 4 chains) and also an internal structure (II) found in type 3 chains. Ab M2 agglutinates all A and AB erythrocytes but does not react with salivary glycoproteins.

Although Landsteiner originally described A, B, and O blood groups on the surface of erythrocytes, it has long been known that these antigens are not confined to red cells but are found in most secretions and in many tissues of the human body (Race & Sanger, 1975). The immunodominant structure for the blood group A determinant, which is one of the most extensively studied specificities, is considered to be

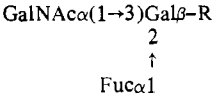

However, it has been found that the remainder of the carbohydrate chain (R) has much influence on the precise specificity of the determinant. Different blood group A variant structures have been described that have different sugars and sugar sequences in the R region (Kabat, 1973; Watkins, 1980; Hakomori, 1981). For example, the A determinants (as well as the B, H, and Lewis determinants) are based on two different carbohydrate sequences, i.e., Galβ(1→3)GlcNAcβ-(1→3)Galβ- or Galβ(1→4)GlcNAcβ(1→3)Galβ-. These structures are designated type 1 and type 2 chains, respectively. More recently, a type 3 chain blood group determinant [extended or repetitive A: GalNAcα(1→3)Galβ(1→3)-GalNAcα(1→3)Galβ(1→4)GlcNAc] and a type 4 A chain based on the globo sequence [GalNAcα(1→3)Galβ(1→3)-GalNAcβ(1→3)Galα(1→4)Gal] have been described (Clausen et al., 1984, 1985).

Following the development of the hybridoma technique, a number of anti-blood group A monoclonal antibodies have

† This work was supported by grants from the National Cancer Institute [CA-34039 and CA-08748 (K.O.L.) and CA-19224 and GM-23180 (S.H.)]. H.C. is supported by the Ingeborg og Leo Dannin Fonden and Vera og Carl Michaelsens Legat, Denmark.
‡ Memorial Sloan-Kettering Cancer Center
§ Fred Hutchinson Cancer Center.
‖ University of Lund.

0006-2960/85/0424-7820$01.50/0